by the exchange reaction. Given the fact that only a minority of the chains are exchanged, a fairly substantial change in N of the reacted macromolecules would lead to a modest change in $[\eta]$ in any case. Therefore, the constancy of R_g is considered more significant evidence that the skeletal chemistry of the HPB is unaffected by the D–H exchange reaction. This point will be checked more thoroughly with techniques such as gel permeation chromatography and melt rheology in future work.

The observation that only a small fraction of the chains are appreciably reacted is something of a surprise, though this probably results from the use of heterogeneous catalyst. We note, however, that a similar product distribution is obtained in analogous deuterium–exchange reactions involving *n*-hexane[13] and *n*-heptane[14] over metal catalysts. Addition reactions, on the other hand, appear to proceed more uniformly; saturation of polybutadiene with either H_2 or D_2 over a heterogeneous palladium catalyst results in quantitative addition to all chains.[9,15] It is clear that more experiments, including those using a deuterated solvent, are needed to improve the yield of labeled chains by exchange. Another point to be investigated is the possible dependence of exchange kinetics on molecular weight, as this would affect interpretation of SANS patterns of polydisperse samples prepared in this manner. Such work is currently under way.

This exchange technique should be applicable to other polyolefins and polymers containing olefinic sequences. The availability of a direct method for obtaining deuterated polymers will significantly expand the power of SANS experiments to study polymeric systems.

Acknowledgment. This research was supported by the Gas Research Institute (Basic Sciences Division, Contract 5081-260-0539). We are indebted to Prof. Robert Burwell, Jr., for sharing with us his considerable experience in heterogeneous catalysis and to C. R. Bartels for assistance with SANS measurements and for many helpful discussions.

References and Notes

(1) Boué, F.; Nierlich, M.; Liebler, L. *Polymer* **1982**, *23*, 29.
(2) Crist, B.; Graessley, W. W.; Wignall, G. D. *Polymer* **1982**, *23*, 1561.
(3) Willenberg, B. *Makromol. Chem.* **1976**, *177*, 3625.
(4) Gradjean, J. *Makromol. Chem.* **1977**, *178*, 1445.
(5) Willenberg, B. *Makromol. Chem.* **1977**, *178*, 2401.
(6) Linder, P. *Makromol. Chem.* **1981**, *182*, 3653.
(7) Kemball, C. In "Advances in Catalysis"; Academic Press: New York, 1959; Vol. 11, pp 223–62.
(8) Burwell, R. L., Jr. *Acc. Chem. Res.* **1969**, *2*, 289.
(9) Tanzer, J. D.; Bartels, C. R.; Crist, B.; Graessley, W. W. *Macromolecules* **1984**, *17*, 2702.
(10) Bartels, C. R.; Crist, B.; Graessley, W. W. *Macromolecules* **1984**, *17*, 2708.
(11) Kostorz, G.; Lovesey, G. In "Treatise on Materials Science and Technology: Neutron Scattering"; Academic Press: New York, 1979; Vol. 15, pp 5–8.
(12) Debye, P. *J. Phys. Colloid Chem.* **1947**, *51*, 18.
(13) Burwell, R. L., Jr.; Shin, B. K. C.; Rowlinson, H. C. *J. Am. Chem. Soc.* **1957**, *79*, 5142.
(14) Forrest, J. M.; Burwell, R. L., Jr.; Shin, B. K. C. *J. Phys. Chem.* **1959**, *63*, 1017.
(15) Rachapudy, H.; Smith, G. G.; Raju, V. R.; Graessley, W. W. *J. Polym. Sci., Polym. Phys. Ed.* **1979**, *17*, 1211.

Deformation Behavior of Styrene–Butadiene–Styrene Triblock Copolymer with Cylindrical Morphology

Tadeusz Pakula,† Kenji Saijo, Hiromichi Kawai,‡ and Takeji Hashimoto*

Department of Polymer Chemistry, Faculty of Engineering, Kyoto University, Kyoto 606, Japan. *Received September 13, 1984*

ABSTRACT: Morphological changes related to deformation of styrene–butadiene–styrene block copolymers with a cylindrical microdomain structure have been studied by small-angle X-ray scattering. The behavior of originally isotropic, solution-cast samples has been compared with the deformation and related structural changes of samples with original macroscopically oriented morphology. The structure related to various stages of deformation has been determined from SAXS patterns by considering separately changes in the single-particle scattering and changes in the lattice factor, both of which influence the scattering patterns. The early and intermediate stages of deformation of the triblock copolymer are controlled by its morphology, while at large extensions the deformation and resulting structure are determined by molecular orientation in the polybutadiene phase.

I. Introduction

Peculiar mechanical properties of triblock styrene–butadiene–styrene (SBS) polymers have been observed by many authors.[1–8] When stretched, in some cases, these polymers initially show a stress–strain dependence similar to those of glassy polymers drawn below the glass transition temperature. Beyond the yield point, however, the SBS polymer becomes rubbery with high elasticity and large recoverable deformation.[4–8] Moreover, after stretching and especially upon annealing after removal of the external stress, the specimens can show a healing effect in that properties of the original undeformed state are recovered.[4–8] Attempts have been made to explain these effects on the basis of structural changes at various stages of deformation. The strain-induced plastic-to-rubber transition in SBS block copolymers has been attributed to fragmentation of the originally rigid structure by large plastic deformation of the glassy component. The healing process has been attributed to the reformation of the original structure.[5–7] The understanding of the deformation mechanism in this type of polymer is, however, still not satisfactory.

Detailed consideration of these effects must take into account the morphology of these polymers, which is highly heterogeneous and ordered on various dimensional levels. Figure 1 shows schematically the cylindrical microdomain

† On leave from the Center of Molecular and Macromolecular Studies, Polish Academy of Sciences Łodz, Poland. Present address: Max-Planck-Institut für Polymerforschung, Mainz, West Germany.
‡ Present address: Hyogo University of Education, Yashiro-cho, Kato-gun, Hyogo-ken 673-14, Japan.

0024-9297/85/2218-1294$01.50/0

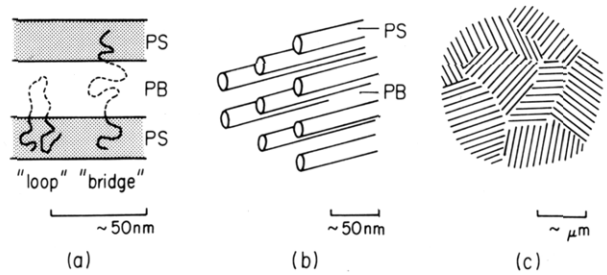

Figure 1. Levels of order in macroscopically isotropic samples of SBS block copolymers with cylindrical microdomain structures: (a) molecular level; (b) submicroscopic level; (c) microscopic level. PS and PB designate polystyrene and polybutadiene microphases, respectively.

structure that can form in this type of block copolymer. The order on the molecular level is caused by microphase separation which takes place due to repulsive interactions between different constituent molecular chains (Figure 1a). As a result the block chains are spatially segregated into microdomains, each containing essentially only one constituent.[9-12] The size of the microdomains and their nearest-neighbor distance are of the order of the unperturbed chain dimensions due to the molecular connectivity of the constituent macromolecules.[9-12]

In SBS block copolymers the ends of the molecular chains form polystyrene microphases while the central parts of the macromolecules build up polybutadiene microphases as illustrated in Figure 1a. Thus the chemical junction points between different block chains are located at the interface. There are two possible chain configurations related to such a structure that are important from the mechanical point of view: (1) the polybutadiene chain can form a "loop" when the polystyrene parts of the same molecule are in the same polystyrene domain, or (2) the polybutadiene chain can form a "bridge" when the styrene ends of the molecule belong to different polystyrene domains. Sizes of domains and their morphology are related to the molecular volumes of the polystyrene and polybutadiene blocks.[9-22] Figure 1 shows the cylindrical microdomains of polystyrene immersed in the polybutadiene matrix. Many experimental studies have shown that the cylindrical microdomains can be spatially ordered, with the same local orientation or even forming a lattice with relatively uniform distances between cylinder axes (Figure 1b).[23-29,31] Such an "ordered microcomposite material" is mechanically highly anisotropic.[26,28-30] The spatial order can extend to macroscopic dimensions under special treatment of the samples.[24,29] In most cases, however, there are ordered regions ("grains") with dimensions of several microns. Generally, adjacent grains have dissimilar orientations of the cylinder axes (Figure 1c) so that samples much larger than the grain dimension are macroscopically isotropic.

If an external force is applied to such a sample, the local stresses and strains will fluctuate considerably according to fluctuations of the local mechanical properties caused by random orientation of the anisotropic structural elements. Hence at a certain stage of macroscopic deformation, the individual grains can be at various local deformation states and the macroscopic mechanical response will be a complex combination of these local mechanical states. The apparent structure of such samples represents an average over the various local structural states.

We have studied the structural changes observed during deformation of initially isotropic samples of SBS block copolymers compared with the behavior of the samples in which the orientation of the cylindrical domains extends uniformly along the whole sample. The oriented samples were deformed parallel, perpendicular, and at 45° to the direction of the initial orientation of the domains. These samples are considered as models of local behavior in the initially isotropic samples.

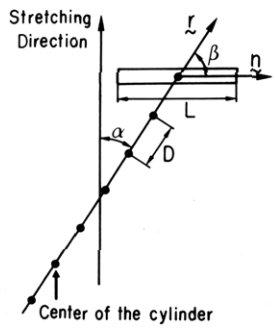

Figure 2. Parameters describing the unidimensional lattice of cylindrical microdomains.

Polymer structure was studied by small-angle X-ray scattering. We first discuss changes in X-ray scattering patterns that can result from structural changes in these polymers.

II. Small-Angle X-ray Scattering from Cylindrical Microdomains

Small-angle X-ray scattering is especially useful in studies of block copolymers in which the dimensions of structural elements are in the range of the highest sensitivity of the technique. There are many procedures[32,33] for analysis of scattering data that permit detailed characterization of polymer morphology. They are, however, primarily applicable to high degrees of order or high degrees of disorder of structural elements.

The morphological changes resulting from deformation of block copolymers are very complex, and many structural parameters (such as sizes of domains, their orientation distribution, and interdomain distances and their relative uniformity) can change simultaneously.[5-7] There are no general methods for drawing quantitative conclusions about all of these changes from the scattering patterns alone. We here discuss qualitatively some effects of structural changes in oriented samples on the shape of scattering patterns that are obtained in highly deformed samples of SBS block copolymers.

Our interpretation is based on a simplified model of a one-dimensional assembly of the cylindrical domains, the orientation and intercylinder distances of which can constitute a kind of unidimensional lattice. We assume that the assembly lies in the plane perpendicular to the incident X-ray beam. The parameters describing such a model are illustrated in Figure 2. We choose the vertical direction as the direction of stretching (SD). The vector $\mathbf{r}$ is parallel to the axis of the unidimensional lattice along which the centers of the cylindrical domains are arranged with a mean identity period of D. The lattice axis $\mathbf{r}$ is generally inclined to SD by an angle α. The orientation of the cylindrical axes $\mathbf{n}$ can be inclined to the lattice axis by an angle β.

It is well-known that the scattered intensity distribution that determines the shape of the observed scattering pattern depends on all these parameters, and their relationship can be described approximately by the equation[33]

$$I \sim \langle f \rangle^2 Z$$

where $\langle f \rangle^2$ denotes a particle-scattered intensity (particle factor) dependent on shape, size, and orientation of individual particles (cylinders), and Z denotes a lattice factor

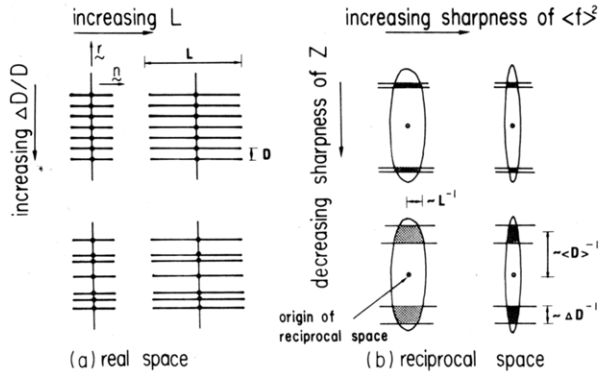

Figure 3. Influence of particle length and interparticle distance of the unidimensional lattice of cylindrical microdomains on the scattering patterns: (a) assumed structures; (b) schematic representation of resulting scattering patterns.

dependent on the interparticle distances.

Figure 3a shows the simplest cases of unidimensional superstructures in which the lattice vector **r** is perpendicular to the particle vector **n** ($\beta = 90°$). Both the particle factor and the lattice factor can change: the first due to the length of the particles (L) and the second due to the fluctuations of the interparticle distances ($\Delta D/D$), the lattice points being shown by dots in the figure. Figure 3b shows schematically changes in scattering patterns that result from changes in these two factors. We represent the scattering from a single particle by an ellipsoid, the axial ratio of which is higher for long, well-developed particles and the long axis of which is oriented perpendicular to the particle orientation. Generally, the scattering intensity associated with the particle factor decreases monotonically with scattering angle at the small angles of interest. The interparticle lattice will give maximum scattering intensity at the angle reciprocally related to the mean distance $\langle D \rangle$ between the centers of the particles along the lattice axis. The scattering maximum associated with Z extends laterally to infinity because of the one-dimensionality. However, dependending on the degree of the lattice distortion, this maximum along the longitudinal direction (parallel to **r**) can be sharp and intensive or broad with a low maximum intensity as represented in Figure 3b by horizontal bands with various widths of the scattering angle intervals related to the first-order interparticle interference maximum. The net scattering pattern I is determined by a product of these two contributions $\langle f \rangle^2$ and Z.

As shown in Figure 3b the shape of the scattering pattern can change according to changes in the structural parameters, and it is possible that some qualitative conclusions about these parameters can be drawn from experimental patterns by analysis of their shapes. A more complex superstructure, in which orientation of the cylindrical domains and lattice axes can change with respect to the stretching direction, is illustrated in Figure 4 together with the expected changes in the scattering patterns. The scattering patterns depend on whether the particle or the lattice factor becomes more sharp. In case A the structure has lattice vector **r** parallel to the stretching direction ($\alpha = 0°$) and particle vector **n** inclined to the lattice vector ($0° < \beta < 90°$). In cases B and C the lattice vectors are inclined to the stretching direction ($0° < \alpha < 90°$) while the particle vectors have particular orientations with respect to the lattice: (1) $\beta = 90°$ and (2) $\beta = \alpha$ for B and C, respectively. As a result in C the particle vector **n** is parallel to the stretching direction. The structures assumed in D and E are identical to those in A and C, respectively, except for the rotation of the lattice vector

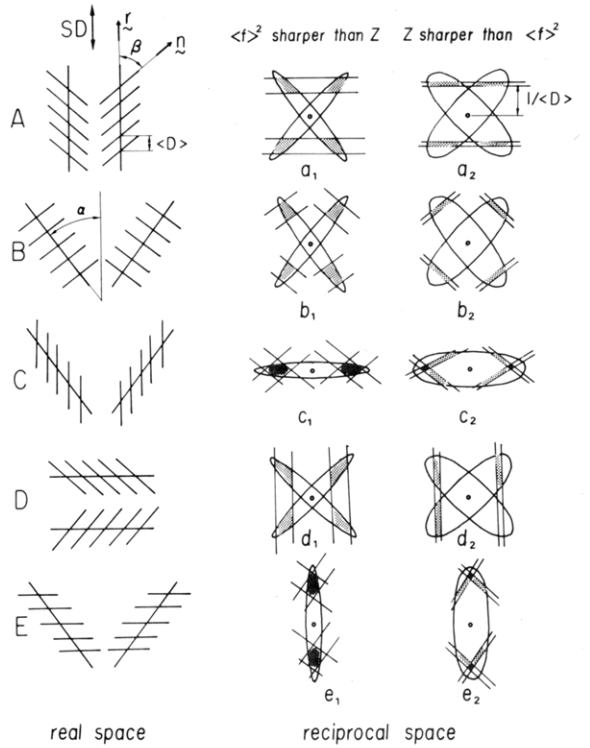

Figure 4. Structures and resulting forms of scattering patterns for various orientations of particles and lattice axes with respect to drawing direction.

r by 90° around the axis perpendicular to the paper. Consequently the corresponding scattering patterns are respectively identical but rotated 90° around the axis perpendicular to the paper. It can be seen that the angular position of the scattering maximum with respect to the scattering angle 2θ, as well as the shape and orientation of the scattering lobes related to the maximum, is dependent on the structural parameters. Positions of the lobes depend on the particle orientation and the average interparticle distance while shapes of the lobes and their orientation depend on the orientation of particles with respect to the lattice axis and on the relative sharpness of the particle and lattice factors. In some cases, the structure can be uniquely identified by comparing the patterns presented in Figure 4 with experimental patterns. For example, the very characteristic case a_2, in which the short particles inclined to the stretching direction form a regular lattice along the deformation direction, gives rise to a scattering pattern with the four lobes elongated in the direction perpendicular to the stretching direction. The schematic patterns in Figure 4 do not consider any orientation fluctuations, which under experimental conditions can influence considerably the observed intensity distribution in the scattering pattern. It is clear that the combined effect of fluctuations of particle orientation within the assemblies and of orientation distribution of lattice axes among the grains make the interpretation of scattering patterns more difficult.

III. Experimental Methods

1. Samples. Two polymers have been studied: (1) research-grade styrene–butadiene–styrene block copolymer, designated TR 41-1648 (Shell Development Co.), with 29.3 wt % polystyrene, total molecular weight $M_v = 110\,000$ (viscosity average), and block molecular weights of styrene, butadiene, and styrene 16, 78, and 16 (in units of thousands), respectively, and (2) the same type of triblock polymer, designated TR 1102 (Shell Development Co.), with 28 wt % of polystyrene and total molecular weight measured by GPC 52 000 (M_n) and 76 000 (M_w).

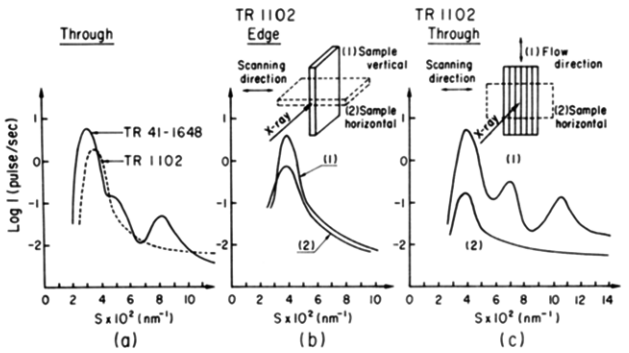

Figure 5. Intensity distributions in SAXS patterns (a) for solution-cast samples of TR 41-1648 and TR 1102 under through-radiation, (b) for solution-cast film of TR 1102 under edge-radiation, and (c) for press-molded sample of TR 1102 under through-radiation.

The isotropic film specimens were obtained by solvent casting from a 10% solution of the polymer in toluene. The films with oriented cylindrical morphology were prepared from polymer TR 1102 by press-molding at 160 °C, the orientation being obtained by shear flow.

For drawing experiments, ribbon-shaped specimens 5 mm wide were cut out from the films, which were about 2 mm thick. Samples of the oriented films were cut out along directions parallel to, perpendicular to, and at 45° to the flow direction of the polymer. It was established as we will show later that the flow direction coincided with the direction of orientation of the cylindrical microdomains.

2. SAXS Measurements. Small-angle X-ray measurements were performed with rapid X-ray detecting system with a rotating-anode X-ray generator and a position-sensitive proportional counter (PSPC).[34,35] Pinhole collimation was obtained with two 0.5-mm pinholes separated by 400 mm. The scattered X-ray intensity distributions were recorded along the horizontal direction 1.154 m from the sample. In order to obtain a true point collimation with identical slit-length and -width weighting functions, we placed a height-limiting slit in front of the PSPC.[34,35] The full-width at half-maximum (fwhm) for the two weighting functions was 1.15 mrad, or 7.2×10^{-3} nm^{-1} in units of s as defined by $(2 \sin \theta)/\lambda_X$ (2θ and λ_X being the scattering angle and X-ray wavelength, respectively), which was sufficiently narrow for our studies (for example, fwhm for TR 41-1648 in Figure 5a is 10×10^{-3} nm^{-1}.)

The sample holder, which was able to rotate around the axis of the incident X-ray beam, will be described elsewhere.[36] Samples stretched to appropriate draw ratios were clamped in the sample holder so that their dimensions did not change during scattering measurements. Scattering intensity distributions were recorded at various orientations of the drawing direction to the horizontal with the film surface perpendicular to the X-ray beam. Intensity distributions corrected for absorption, air scattering, and background scattering were used for construction of the two-dimensional scattering patterns represented by contour lines of equal intensity. In Figures 8 and 9 the measured intensity distributions are shown by three contour lines of equal intensity with 5, 1, and 0.1 pulses/s (at relative intensity levels). The scattering intensity distributions are divided into four differently hatched regions with the three contour lines as the borders: regions with intensity higher than 5.0 pulses/s, those with intensity between 5.0 and 1.0 pulses/s, those with intensity between 1.0 and 0.1 pulse/s, and those with intensity less than 0.1 pulse/s. All X-ray scattering measurements were performed at room temperature.

IV. Results

1. Structure of Undrawn Samples. The undrawn films cast from solution had the cylindrical microdomains randomly oriented in the plane parallel to the film surface. When the incident X-ray beam was normal to the film surface (designated hereafter as "through-radiation"), the scattering intensity distributions were circularly symmetric about the incident beam axis. Identical intensity distributions were obtained from various regions of the samples.

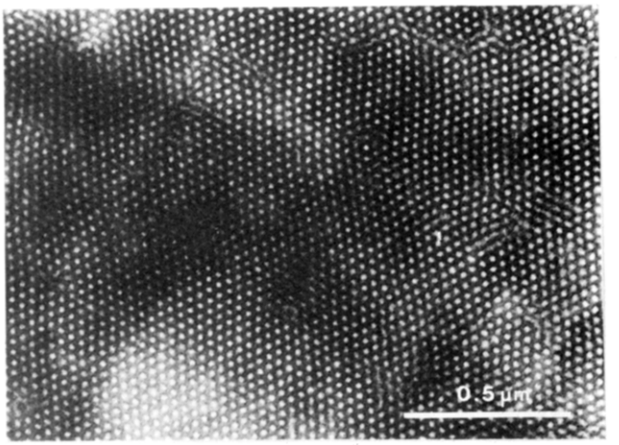

Figure 6. Electron micrograph of macroscopically oriented domains in press-molded samples of TR 1102.

The intensity distributions for both polymers studied under through-radiation are shown in Figure 5a. For both polymers, however, a preferential orientation of the microdomains was observed when the scattering was recorded with the incident beam parallel to the film surface ("edge-radiation").

Scattering intensity distributions from polymer TR 1102 recorded at horizontal and vertical film positions are shown in Figure 5b, indicating that the cylindrical domains are preferentially oriented with their axes **n** in planes parallel to the film surface.

Figure 5c shows the scattering intensity distributions for polymer TR 1102 recorded with the incident beam perpendicular to the film surface and at two sample positions: (1) the flow direction vertical, and (2) the flow direction horizontal. The results indicate a preferential orientation of the microdomains along the flow direction of the polymer during film preparation. The presence of three maxima on the scattering curve with relative positions at scattering angles proportional to 1, $\sqrt{3}$, and $\sqrt{7}$, respectively, indicate a hexagonal packing of the microdomains. Nearly hexagonal packing of the microdomains was also observed for an isotropic sample of TR 41-1648 (Figure 5a). The two polymers differ in molecular weight, which results in differences in the interdomain distances. The values of the identity periods (Bragg spacings) determined from the position of the first-order maxima in scattering intensity distributions presented in Figure 5 are 335 Å for TR 41-1648 and 284 and 255 Å for isotropic and oriented samples of TR 1102, respectively. The good orientation of the cylindrical domains in press-molded samples was also shown by electron microscopy (Figure 6).

2. Mechanical Behavior. Figure 7a shows the stress–elongation curves for isotropic samples of the two polymers stretched at room temperature at a constant drawing rate of 2 cm/min. The stress is the nominal stress, i.e., the drawing force divided by the cross-sectional area of the undrawn sample.

Figure 7b shows the tensile stress–elongation behavior of TR 1102 with an originally oriented cylindrical domain structure, recorded for samples drawn in three different directions with respect to the microdomain orientation under the same conditions used for the isotropic samples. A sharp yield point is observed for the sample with the domains oriented along the drawing direction, and the yield stress has the highest value but the elongation at the yield point is the smallest. The stress at elongations close to the yield point is much smaller for the samples with the domains oriented at 45° and perpendicular to the drawing direction. The stress–strain curves intersect, however, at

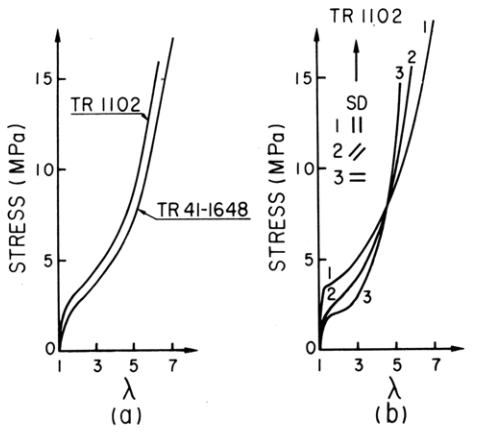

Figure 7. Stress–strain dependence for (a) solution-cast samples and (b) press-molded samples deformed in various directions with respect to microdomain orientation. Curves 1, 2, and 3 correspond to those deformed parallel, at 45°, and perpendicular to the orientation of the cylinders.

higher elongations (the one point of intersection presented here is accidental), and above this point the highest stress is needed to deform samples in which the domains were originally perpendicular to the drawing direction. We will show later that at low elongation (λ) the orientation and deformation of the domains control the mechanical behavior but at high elongation the orientation and deformation of the chain molecules comprising the domains control the behavior.

3. Structural Changes Related to Deformation. Scattering patterns recorded at various elongations at room temperature for originally isotropic samples of TR 41-1648 and TR 1102 are shown in parts a and b of Figure 8, respectively. The stretching direction is vertical and the numbers by each pattern indicate the draw ratio at which the scattering was recorded. The patterns for the two polymers change similarly with extension and, moreover, this change is similar to that observed previously for a triblock copolymer with a lamellar structure.[6,7]

At small deformations, the meridional scattering maximum related to the microdomains originally oriented perpendicular to the stretching direction shifts to smaller angles, which means that the interdomain distance has increased along the stretching direction. At the same time its intensity decreases, which can be attributed to increasing disorder in interdomain distances or to reorientation of the microdomains from the direction perpendicular to the stretching direction. At elongations close to the yield point the maximum in the meridional direction disappears, indicating that almost all microdomains originally oriented perpendicular to the stretching direction have changed their orientation. At these elongations also the maximum in the euatorial position, related to microdomains originally oriented along the stretching direction, starts to decrease and it disappears at elongations greater than 100%. This result indicates that the domains originally oriented along the stretching direction have changed their orientation or that the interdomain correlation in such oriented regions has been destroyed during yielding.

At higher elongations the well-developed four-point pattern is observed, indicating that the microdomains assume preferential orientations inclined to the stretching direction. Details of these patterns change however with increasing deformation; i.e., the scattering lobes change their shapes and orientations. These changes, according to the discussion presented in section II, can be caused by changes in particle length and orientation and by changes

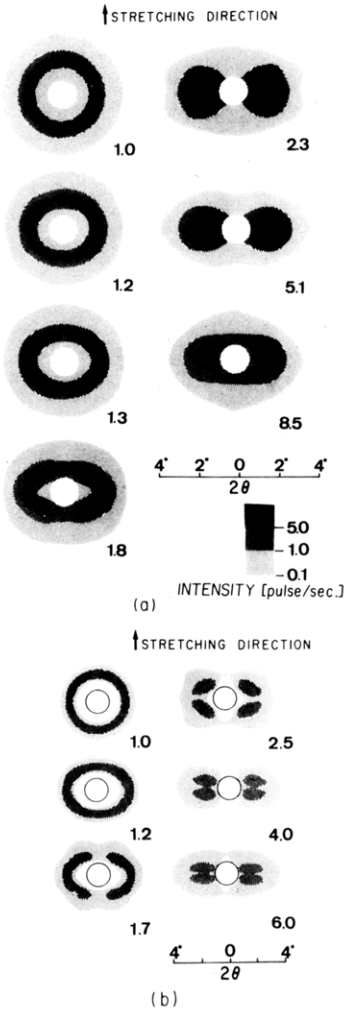

Figure 8. SAXS patterns at various draw ratios of deformed samples of (a) TR 41-1648 and (b) TR 1102. The numbers designate the draw ratios.

in orientation and perfection of the local interparticle lattice. For example, the patterns recorded at elongations $\lambda = 2.3$ for TR 41-1648 (Figure 8a) and $\lambda = 2.5$ for TR 1102 (Figure 8b) can be compared to example b_2 in Figure 4, in which the short cylindrical microdomains form a lattice perpendicular to the particle orientation ($\beta = 90°$) but the lattice axes are inclined to the stretching direction by the angle $\alpha \approx 30°$. At higher deformations, $\lambda = 5.1$ for TR 41-1648 and $\lambda = 4$ or $\lambda = 6$ for TR 1102, the scattering patterns can be compared to example a_2 in Figure 4. Here the lattice axes become parallel to the stretching direction ($\alpha = 0°$) but the short microdomains are inclined to that direction by the angle $\beta \approx 20°$.

Finally, at elongations close to fracture all maxima in the scattering pattern disappear. This range of deformation and the related scattering patterns were not observed in cases when the sample underwent fracture at smaller deformations, probably because of some type of inhomogeneity not related to the morphology.

An unequivocal identification of these changes in scattering patterns with structural changes is difficult for the initially isotropic samples, which have the grain structure shown in Figure 1c. It is obvious that the grains oriented at various directions to the drawing direction behave differentialy under applied stress and that the observed scattering patterns represent integrated information about all structural changes taking place in the sample.

As a model of local behavior in such samples we used specimens with a macroscopically oriented structure.

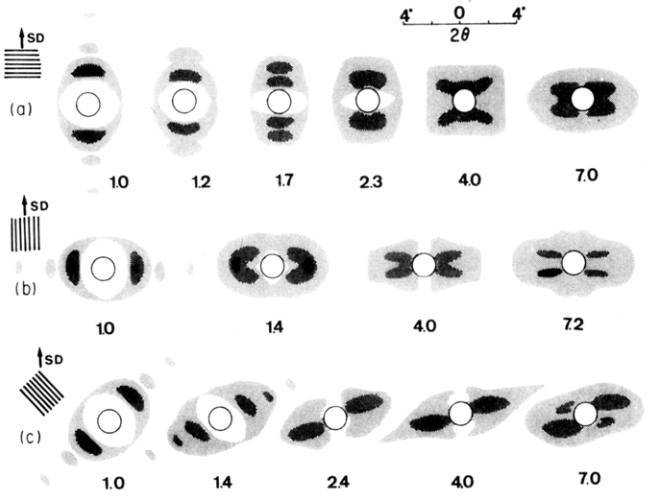

Figure 9. SAXS patterns at various deformations of press-molded samples of TR 1102 stretched perpendicular (a), parallel (b), and at 45° (c) to the original orientation of the cylindrical microdomains. The numbers designate draw ratios.

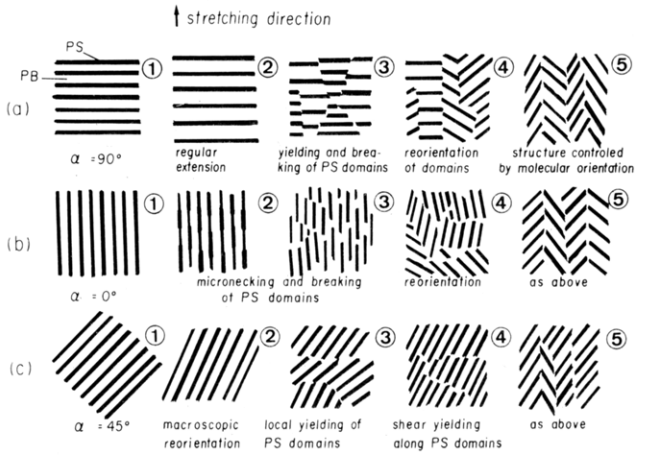

Figure 10. Schematic representation of structural changes caused by deformation of originally oriented SBS polymer with the cylindrical microdomains: (a) SD perpendicular, (b) SD parallel, and (c) SD at 45° to the original orientation of the cylindrical domains.

Figure 9 shows three series of scattering patterns recorded under deformation of such samples with various orientations of the original cylindrical microdomains to the drawing direction. In all cases the drawing direction is vertical.

The first series patterns, Figure 9a, is related to deformation of samples in which the cylindrical domain structure (**n**) is oriented perpendicular to the applied force. The initial scattering has maximum intensity in the meridional direction. At small deformations all three maxima indicating hexagonal packing of the microdomains shift to smaller scattering angles. However, their relative intensities remain nearly constant, which means that the correlation of the interdomain distances does not change under this small deformation except for a uniform expansion of the mean interdomain distance along the stretching direction and that the rubbery matrix is deformed almost homogeneously. This change of structure is depicted schematically in Figures 10a (from 1 to 2) and 11a,b. The deformation behavior changes when the sample reaches the yield point on the stress–strain curve (compare Figure 7b), probably related to yielding in the polystyrene phase. The scattering pattern recorded at this deformation range ($\lambda = 1.7$ in Figure 9a) shows two distinct maxima of approximately equal intensity at two different

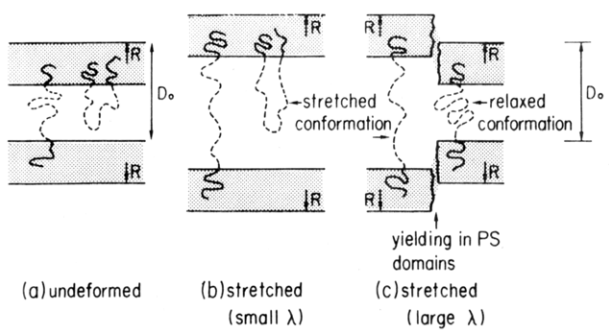

Figure 11. Effect of yielding of polystyrene domains originally perpendicular to the stretching direction.

scattering angles but still in the meridional direction. The maximum at smaller angles is related to the first-order maximum in the original scattering pattern but its position is shifted toward smaller angles with increasing deformation, consequently suggesting increased interdomain distance. The strong second-order maximum appears when the sample passes through the yield point on the stress–strain curve and seems to indicate that the deformation of some localized regions in the sample has relaxed (see parts b and c of Figure 11). The position of this maximum is almost the same as that of the first-order maximum in the original undeformed sample, which means that the original interdomain distance has been restored in these regions. It can be supposed, as shown in Figure 11c, that yielding in the polystyrene domains takes place along a direction nearly perpendicular to the cylindrical domain axis **n**. At these deformations the domains remain perpendicular to the drawing direction. It is, however, supposed that the initial structure may be fragmented into smaller regions within which the local deformation can differ considerably. These fragmented domains can now change their orientation more easily, as observed in scattering patterns for samples subjected to large deformations, e.g., the pattern for $\lambda = 4$ (compare pattern a_1 in Figure 4). The lateral compression of the sample during uniaxial stretching is believed to cause this reorientation of the domains. From the arguments in Section II (e.g., Figure 4) it may be concluded that despite changes in the orientation of the domains the distances between them remain correlated along the drawing direction at all deformations, as shown in A, Figure 4. In other words, the unidirectional lattice vector **r** remains parallel to the stretching direction. This effect is also observed in the last scattering pattern in this series (Figure 9a, $\lambda = 7.0$), which may be compared to the example a_2 in Figure 4 in which the lattice vector **r** is oriented along the drawing direction but the particle vector **n** is oriented at some small angle to the drawing direction. The structural changes described here are illustrated schematically in Figure 10a.

Samples with the microdomains oriented initially along the deformation direction behave differently (Figure 9b). The hexagonal packing of the microdomains is preserved only at very small deformations. After yielding, i.e., at λ greater than 1.1, an intensive equatorial scattering is observed at scattering angles greater than the position of the first-order maximum in the original scattering pattern. The related Bragg spacing determined from the pattern recorded at $\lambda = 1.4$ is smaller than the original spacing by a factor of 0.84, which is almost the same as the change in the lateral dimensions of the deformed sample: $d/d_0 = 0.83$. This result means that in spite of the yielding process the local change in dimensions related to microdomain structure is the same as the macroscopic deformation. In fact, macroscopic necking was not observed,

which indicates a homogeneous deformation in the whole sample. The shape of the scattering pattern recorded at $\lambda = 1.4$ can be compared to the predicted case c_2 in Figure 4 for which the cylindrical microdomains oriented along the stretching direction form lattices with lattice axes **r** inclined to the deformation direction by an angle α. This type of structure produces a scattering pattern with intensive equatorial scattering and V-shaped lobes. Accordingly, we suggest that at this stage of deformation the cylindrical polystyrene domains that were originally oriented along the stretching direction undergo local yielding which results in both micronecking and breaking up of the cylindrical domains in such a way that their yielded and nonyielded parts form lattices with the lattice vector **r** oriented at $\alpha = 30°$ to the stretching direction. A structural model of such changes is shown Figure 10b-2. we suggest that the micronecking or breaking up of polystyrene cylinders goes on in a correlated way along "slip lines" oriented 30° to the stretching direction. This type of structure can be seen in electron micrographs reported by Odell and Keller[28] for similar samples deformed above the yield point.

As the deformation increases further the equatorial scattering becomes weak and a four-point pattern appears ($\lambda = 4$ in Figure 9b), which indicates a reorientation of microdomains from their original direction. At the final state of drawing the microdomains are inclined to the drawing direction by a small angle (Figure 9b, $\lambda = 7.2$) The interdomain lattice orientation (vector **r**) has changed from a direction perpendicular to the domain orientation in the original sample to one parallel to the drawing direction in samples deformed to $\lambda > 7$. The scattering pattern obtained at this state corresponds to that shown in Figure 4 a_2, for which the lattice factor has a sharper intensity distribution along the drawing direction than the intensity distribution of the particle factor. In this example the orientation of amorphous polybutadiene blocks is initially normal to the stretching direction but becomes parallel to the stretching direction. The orientation of these polybutadiene chains, along which mechanical energy is transmitted through the sample, is probably related to the observed disorientation of the fragmented polystyrene microdomains, leading to the structure shown schematically in the last column of Figure 10b.

In samples in which the microdomains are oriented 45° to the drawing direction the main effect at lower deformation results from homogeneous reorientation of the original structure by a shearing mechanism in the polybutadiene phase. The maxima in scattering patterns related to hexagonal packing of the microdomains (Figure 9c) are observed up to relatively high extension ratios. At deformations greater than 100% the intensity distribution becomes broader in both the tangential and radial directions, suggesting that the cylinders undergo fragmentation and inhomogeneous reorientation as well as inhomogeneous deformation of their spacings. This result could be caused by local yielding as in the case of samples with cylindrical domains originally perpendicular to the drawing direction (Figure 11). At higher deformation ($\lambda = 4$) intensive scattering maxima are observed, indicating better local alignment of the domains, which, in turn, can be attributed to possible plastic shear deformation of the polystyrene domains. The orientation of the scattering lobes indicates that the interlamellar lattice vector is at first almost perpendicular to the domain orientation but becomes almost parallel to the deformation direction (Figure 10c), as is the case in the final deformation state of samples drawn parallel or perpendicular to the cylinder axes except that the deformation at 45° lacks the symmetry in the orientation of the cylinder axes with respect to the drawing direction.

All the structural changes attributed to the observed scattering patterns for initially oriented samples are shown schematically in Figure 10.

V. Discussion

We have presented a variety of deformation behaviors that occur when the oriented microdomain structure is deformed at various angles to its original orientation. The structural changes that differ substantially among these samples were observed at low deformations where yielding, fragmentation, and reorientation of the domains take place. The detailed nature and the sequences of these processes are strongly dependent on the orientation of the stretching force to that of a "submicroscopic composite" composed of hard cylindrical domains of polystyrene embedded in the rubbery polybutadiene matrix. Some of the effects observed can be understood in terms of the mechanical properties of an oriented two-component system. For example, it is obvious that a system with domains oriented along the drawing direction will behave initially like a simple mechanical model of two different phases connected in parallel. In such a model most stresses are transmitted along the phase with the higher elastic modulus, and this is why the stress required for plastic flow in the polystyrene phase is reached in such samples at very small deformations. On the other hand, samples with microdomains perpendicular to the drawing direction will behave like a series connection of the different phases, and a higher deformation is needed to produce the stress needed for plastic deformation of the polystyrene phase. Thus the deformation behavior at low elongations is controlled mainly by the morphology of the sample.

In contrast to the differences in behavior of various samples at low and intermediate deformations, the structural state reached at high deformation is almost the same for all samples. In all cases the four-point scattering pattern was observed with the scattering lobes of intensity maxima elongated along the equatorial direction. According to our analysis of scattering patterns, this indicates that the short cylindrical microdomains inclined at $\beta = 20°$ to the draw direction form a lattice oriented along the drawing direction. The explanation for this kind of structure in all highly drawn samples, independent of the original orientation morphology with respect to the draw direction, has to take into account two factors that can influence the deformation mechanism and the final morphology: (1) the system is a composite of two microphases with highly different mechanical properties and with the elements of the dispersed phase highly elongated (cylindrical microdomains of glassy polystyrene in a rubbery polybutadiene matrix), and (2) the polystyrene domains can be connected by "bridge" polybutadiene block molecules which at high extensions will transmit most of the mechanical forces between neighboring polystyrene domains.

If the morphological factor were to control the deformation at both low and high elongations, the expected final structure in highly drawn samples would comprise fragmented cylindrical microdomains of polystyrene oriented with the cylinder axes along the drawing direction. Such morphology has been predicted and observed in highly drawn composite materials with fibrillar inclusions. The observed morphology of highly drawn block copolymer samples is, however, completely different and shows that the final stage of drawing is controlled by the molecular orientation of polybutadiene block molecules. When these

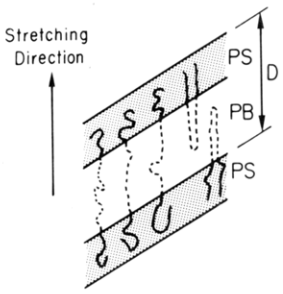

Figure 12. Structure of highly stretched states of SBS block polymer with cylindrical domains.

Table I
Comparison of the Macroscopic Deformation with the Deformation in Lattice Constant Determined from SAXS Measurements[a]

original sample	D_0, Å	λ	$\langle D\rangle/\langle D_0\rangle$
TR 41-1648, isotropic	335	6	4.7
TR 1102, isotropic	284	6	4.6
TR 1102, domains perpendicular to SD	255	7	4.0
TR 1102, domains parallel to SD	255	7.2	2.96
TR 1102, domains 45° to SD	255	7	3.24

[a] D_0 is the identity period (Bragg spacing) of the original structure, D is the lattice constant along the stretching direction (SD) in drawn samples, and λ is the macroscopic draw ratio.

are oriented along the drawing direction, they will cause the positional correlation between polystyrene domains (vector **r**) along the drawing direction, which excludes the orientation of domains (vector **n**) along this direction. The resulting structure is shown schematically in Figure 12, which is a magnification of the final morphological states in Figure 10. From the scattering patterns related to such morphology the mean lattice constant $\langle D\rangle$ can be determined, and its ratio to the original interdomain distance $\langle D_0\rangle$ gives information about the microscopic deformation (Table I). The microscopic extension $\langle D\rangle/\langle D_0\rangle$ is in all cases smaller than the macroscopic deformation, indicating that nonaffine and inhomogeneous deformation probably results from plastic flow in the polystyrene phase and fragmentation of PS domains. This leads to increasing number and decreasing size of PS domains and is probably associated with displacement of the junction points between the constituent block chains along the interface.

It is reasonable to suppose that the effects of plastic flow in the polystyrene phase and elastic extension of polybutadiene chains contribute differently to the final extension, depending on the initial orientation of cylindrical domains with respect to the drawing direction. For example, when the cylindrical domains are oriented initially along the drawing direction, the large plastic deformation of the polystyrene domains is observed at early stages of deformation, but the final extension of the polybutadiene chains approximated by the ratio $\langle D\rangle/\langle D_0\rangle$ (=2.36) is relatively small. On the other hand, when the cylinders are originally perpendicular to the drawing direction, the local plastic deformation is related only to fragmentation of polystyrene domains (Figure 10-3) and the PB chain extension in the final state is higher ($\langle D\rangle/\langle D_0\rangle$ = 4.0). In our opinion these two factors, the plastic deformation of PS domains and the elastic extension of PB chains, account for the intersection of the stress–strain curves presented in Figure 7b.

Comparison of the scattering patterns recorded at large deformations for originally oriented samples (Figure 9) with those for originally isotropic samples (Figure 8) shows that in the latter the morphology of the final drawn state is similar to that for the former. Evidently molecular orientation determines the large deformation state in originally isotropic samples.

At the early stage of deformation in the originally isotropic samples, all the effects observed in originally oriented samples probably take place at once with a statistical distribution that depends on the local initial orientation of individual grains. However, the lengths (L) of the microdomains are limited by the grain size, and it is probable that the reorientation of the grains, which is related to both rotation of the lattice vector **r** and the particle vector **n**, is more significant than in the originally oriented samples. The scattering patterns recorded at intermediate deformations of initially isotropic samples (λ = 2.3 in Figure 8a and λ = 2.5 in Figure 8b) correspond to the pattern b_2 in Figure 4, indicating that the interdomain distances are not correlated along SD but are inclined to it by the angle α (compare cases a_2 and b_2 in Figure 4).

In the originally isotropic samples the microdomains of limited lengths do not need to be fragmented for reorientation and therefore the plastic deformation of the polystyrene domains makes little contribution to the macroscopic deformation compared with originally oriented samples and may involve higher elastic extension of the polybutadiene chains. In fact the extension of polybutadiene chains indicated by the ratio $\langle D\rangle/\langle D_0\rangle$ is relatively high for such samples as shown in Table I.

VI. Conclusions

SBS block copolymers at small deformations behave as typical composite materials in which the morphology and properties of the microphase control the mechanical behavior. At high deformations, however, the orientation of the molecules, which originates from the *molecular connectivity* of the constituent polymers forming the microdomains, controls the mechanical behavior and final morphological state, in contrast to *physical composites*.

Acknowledgment. T.P. is grateful to the Japan Society for the Promotion of Sciences for kindly providing the fellowship in Japan which made it possible for him to perform this study. We are grateful to Prof. Dr. M. Kryszewski, Center of Molecular and Macromolecular Studies, Polish Academy of Sciences, Łodz, Poland, for his encouragement, and to Dr. H. Hasegawa, in our laboratory, for helpful discussions and assistance. This work was partially supported by scientific grants from the Asahi Glass Foundation for Industrial Technology, Japan.

References and Notes

(1) Beecher, J. F.; Marker, L.; Bradford, R. S.; Aggarwal, S. L. *J. Polym. Sci., Part C* **1969**, *No. 26*, 117.
(2) Henderson, J. F.; Grundy, K. H.; Fischer, E. *J. Polym. Sci., Part C* **1968**, *No. 16*, 3121.
(3) Fischer, E.; Henderson, J. F. *J. Polym. Sci., Part C* **1969**, *No. 26*, 149.
(4) Akovali, G.; Niinomi, M.; Diamant, J.; Shen, M. *Polym. Prepr., Am. Chem. Soc., Div. Polym. Chem.* **1976**, *17*, 560.
(5) Hong, S. D.; Shen, M.; Russell, T.; Stein, R. S. In "Polymer Alloys"; Klempner, D., Frisch, K. C., Eds.; Plenum: New York, 1977.
(6) Fujimura, M.; Hashimoto, T.; Kawai, H. *Rubber Chem. Technol.* **1978**, *51*, 215.
(7) Hashimoto, T.; Fujimura, M.; Saijo, K.; Kawai, H.; Diamant, J.; Shen, M. *Adv. Chem. Ser.* **1979**, *No. 176*, 257.
(8) Kotaka, T.; Miki, T.; Arai, K. *J. Macromol. Sci.—Phys.* **1980**, *B17* (2), 303.
(9) Inoue, T.; Soen, T.; Hashimoto, T.; Kawai, H. *J. Polym. Sci., Part A-2* **1969**, *7*, 1283.
(10) Meier, D. J. *J. Polym. Sci., Part C* **1969**, *26*, 81.
(11) Helfand, E.; Wasserman, Z. R. *Macromolecules* **1976**, *9*, 879.
(12) Hashimoto, T.; Shibayama, M.; Kawai, H. *Macromolecules* **1980**, *13*, 1237.
(13) Hashimoto, T.; Fujimura, M.; Kawai, H. *Macromolecules* **1980**, *13*, 1660.

(14) Hoffmann, M.; Kämpf, G.; Krömer, H.; Pampus, G. *Adv. Chem. Ser.* **1971**, *No. 99*, 351.
(15) Helfand, E.; Wasserman, Z. R. *Macromolecules* **1978**, *11*, 960.
(16) Helfand, E.; Wasserman, Z. R. *Macromolecules* **1980**, *13*, 994.
(17) Noolandi, J.; Hong, K.-M. *Ferroelectrics* **1980**, *30*, 117.
(18) Hadziioannou, G.; Skoulios, A. *Macromolecules* **1982**, *15*, 258.
(19) Richards, R. W.; Thomason, J. L. *Macromolecules* **1983**, *16*, 982.
(20) Bates, F. S.; Berney, C. V.; Cohen, R. E. *Macromolecules* **1983**, *16*, 1101.
(21) Hashimoto, T.; Shibayama, M.; Kawai, H. *Macromolecules* **1983**, *16*, 1093.
(22) Shibayama, M.; Hashimoto, T.; Kawai, H. *Macromolecules* **1983**, *16*, 1434.
(23) Kämpf, G.; Krömer, H.; Hoffmann, M. *J. Macromol. Sci.—Phys.* **1972**, *B6* (1), 167.
(24) Dlugosz, J.; Keller, A.; Pedemonte, E. *Kolloid-Z. Polym.* **1970**, *242*, 1125.
(25) Odell, J. A.; Dlugosz, J.; Keller, A. *J. Polym. Sci., Polym. Phys. Ed.* **1976**, *14*, 861.
(26) Folkes, M. J.; Keller, A. In "The Physics of Glassy Polymers"; Haward, R. N., Ed.; Applied Science Publishers Ltd.: London, 1973.
(27) Gallot, B. *Adv. Polym. Sci.* **1978**, *29*, 85.
(28) Odell, J. A.; Keller, A. *Polym. Eng. Sci.* **1977**, *17*, 544.
(29) Mathis, A.; Hadziioannou, G.; Skoulios, A. *Polym. Eng. Sci.* **1977**, *17*, 570.
(30) Folkes, M. J.; Keller, A. *Polymer* **1971**, *12*, 222.
(31) Mori, K.; Hasegawa, H.; Kawai, H.; Hashimoto, T., to be submitted to *Macromolecules*.
(32) Guinier, A.; Fournet, G. "Small-Angle Scattering of X-rays"; Wiley: New York, 1955.
(33) Hosemann, R.; Bagchi, S. N. "Direct Analysis of Diffraction by Matter"; North-Holland Publishing Co.: Amsterdam, 1962.
(34) Hashimoto, T.; Suehiro, S.; Shibayama, M.; Saijo, K.; Kawai, H. *Polym. J.* **1981**, *13*, 501.
(35) Fujimura, M.; Hashimoto, T.; Kawai, H. *Mem. Fac. Eng., Kyoto Univ.* **1981**, *43*, 224.
(36) Pukuła, T.; Saijo, K.; Hashimoto, T. *Macromolecules*, in press.

Dynamic Mechanical Relaxations in Polyethylene

Yash P. Khanna,* Edith A. Turi, and Thomas J. Taylor

Corporate Technology, Allied Corporation, Morristown, New Jersey 07960

Virgil V. Vickroy and Richard F. Abbott

Plastics and Functional Chemicals Division—Chemical Sector, Allied Corporation, Baton Rouge, Louisiana 70892. *Received August 13, 1984*

ABSTRACT: The influence of key physicochemical variables such as density, molecular weight, branching, and thermal history on the dynamic mechanical behavior of polyethylene has been studied. On the basis of our own results and the subject literature, the mechanisms for the α-, β-, and γ-relaxation processes are reviewed. The mechanism of α-relaxation appears to be well established; i.e., it is due to motions of the interfacial regions (tie molecules, folds, loops, etc.) which require chain mobility in the crystal as a precursor and its temperature depends solely on the crystallite (lamellae) thickness. Our results on β-relaxation suggest it to be a glass transition. The γ-relaxation process involves the motion of a short polymer segment (e.g., three to four CH_2) belonging to the bulk amorphous fraction and the chain ends within the crystalline or amorphous phases. The data on energy dissipation and stiffness for various polyethylenes are also presented.

Introduction

Recently we have had applied dynamic mechanical analysis (DMA) to polyethylene in order to understand or explain the product behavior in applications. Interpretation of dynamic mechanical properties of polyethylene in the literature, however, has been quite controversial. Not only the interpretation of dynamic mechanical behavior but also the published data differ because of differences in instrumentation, experimental conditions, sample history, etc. A study[1] was, therefore, undertaken to have a better understanding of the dynamic mechanical properties of polyethylene and, subsequently, to use these results for defining structure/property relationships and relate them to the product performance. Apparently, a somewhat related study by Popli et al.[2] was under way and has appeared in the literature recently. These authors have presented an update of the controversial literature on the mechanical relaxations in polyethylene and, therefore, we will not bring up all the previously reported data. Although Popli et al. discussed only the α- and β-relaxations, we have studied γ-relaxation as well in addition to the viscoelastic properties of polyethylene in the solid state. Preliminary results of our study have appeared elsewhere.[3]

In this manuscript we discuss the dynamic mechanical properties of polyethylene in the light of our results and the subject literature. Accordingly, the mechanisms responsible for the three major, α-, β-, and, γ-relaxations are proposed.

Experimental Section

Materials. The following eight samples were selected for this study:

sample no.		description	source
1	LDPE	linear, LL-1001	Exxon
2	LDPE	conventional NBS 1476	NBS
3	HDPE	high molecular weight, Lot 90449	Hercules
4	HDPE	6097	Union Carbide
5	HDPE	Paxon 4100, Lot 273908	
6	HDPE	Paxon 4100, Lot 293922	
7	HDPE	Milk-Bottle Grade	Allied
8	HDPE	Milk-Bottle Grade	

Sample Preparation. Except for IR and NMR, all the experimental work was carried out on molded samples. Square pieces measuring 2 in. × 2 in. and about 50-mil thickness were compression molded. Thermal history was varied as follows:

Samples 1–8 were molded and then *slow cooled* in the molding press to maximize the crystalline content. A portion of the slow-cooled samples 1, 2, 3, and 8 was subsequently *annealed* under vacuum in an oven for 25 h at 70 and 100 °C. Except for samples 4 and 6, all samples were also *quenched* in water from

0024-9297/85/2218-1302$01.50/0